JOURNAL OF PROPULSION AND POWER
Vol. 17, No. 6, November–December 2001

Multidisciplinary Optimization of Airbreathing Hypersonic Vehicles

Kevin G. Bowcutt*
The Boeing Company, Long Beach, California 90807-5309

Airbreathing hypersonic aircraft and missiles are characterized by a high degree of interdependence between airframe and engine. For nonaxisymmetric vehicles the propulsion system exerts a major influence on vehicle lift and pitching moment; this in turn influences vehicle stability, control, and overall mission performance. Because of strong interactions between the airframe and engine, conceptual design of this class of vehicle requires a multidisciplinary design optimization (MDO) process that can simultaneously account for the impact of selected geometric variables on all vehicle subsystems. This paper describes the development and implementation of an MDO design system that combines propulsion and external aerodynamic forces, mass properties and internal volumetric modeling, and performs geometric optimization of a hypersonic cruise missile to maximize overall mission range. The result is a configuration with range 46% greater than the initial baseline. Such a dramatic performance increase is indicative not only of the power of optimization, but of the difficulty in configuring hypersonic vehicles to synergize the interaction of all vehicle components without MDO methods.

Nomenclature

D	=	drag
g	=	gravitational acceleration
I_{sp}	=	specific impulse
I_{yy}	=	pitch moment of inertia
K	=	centrifugal relief factor
L	=	lift
L_p	=	propulsive lift
ℓ_{chine}	=	chine length
ℓ_{cowl}	=	nozzle cowl length
M_α	=	pitching-moment derivative
$\dot{q}$	=	pitch acceleration
R	=	range
r_E	=	Earth's radius
T	=	thrust in flight direction
$\tilde{T}$	=	thrust magnitude
T_2	=	time to double
V	=	velocity
W	=	weight
W'	=	weight modified by centrifugal relief
$\tilde{W}$	=	required cruise aerodynamic lift
w_f	=	fuel flow rate
x_{eng}	=	engine axial location
α	=	angle of attack
θ_{cant}	=	engine cant angle
θ_{nose}	=	upper-body nose angle
θ_T	=	thrust vector angle

Introduction

IT is difficult in practice to achieve the performance potential promised by hypersonic vehicles that employ scramjets and high lift-to-drag aerodynamics; to do so requires a design process that accounts for all vehicle component interactions and utilizes optimization techniques. A good illustration of this design complexity is provided by a propulsion integration example. For hypersonic vehicles much of the vehicle forebody forms an external inlet compression surface, and the aft boattail serves as a nozzle expansion surface. For asymmetric vehicles the resulting propulsive lift and pitching moment profoundly influence longitudinal trim, which can substantially degrade system performance below that promised by the simple sum of individual components. In addition, component interactions are complex (i.e., highly nonlinear), leading to design solutions that are counterintuitive and almost impossible to arrive at using intuitive design rules and classical one-parameter-at-a-time trade studies. However, by allowing adequate degrees of freedom (design parameters) in a design, creating models that define the performance and physical attributes of major system elements with high fidelity, and applying optimization techniques that identify the best combination of design parameters, delivered system performance can approach ideal values.

In practice, optimization of a vehicle configuration (here referring to external geometry) requires consideration of the interrelations of several geometric variables simultaneously, and it must provide for assessment of all relevant impacts on the vehicle. Often, two or more geometric variables will act in synergy to produce an effect opposite what they would produce alone. As will be shown, multidisciplinary design optimization (MDO), by its consideration of these synergies, can be more effective than single-variable trade studies.

This paper describes recent developments and results of work in hypersonic vehicle MDO. It builds upon past work conducted by the author during the National Aerospace Plane (NASP) program[1] and reported in simplified form.[2] The author's past work focused on single-point performance optimization (i.e., at a single flight Mach and altitude) and included the effects of vehicle aerodynamics, propulsion, and longitudinal trim. The current work optimizes vehicle performance across an entire airbreathing trajectory (specified by Mach vs altitude) that has both acceleration and cruise legs and includes the effects of aerodynamics and propulsion; longitudinal trim, stability and control; and mass properties and volume. An analytic description of vehicle geometry is employed to accommodate prediction of aerodynamic, propulsion, mass property, and volumetric characteristics. Supersonic aerodynamic forces and moments are predicted using shock-expansion theories. Installed engine performance parameters are generated using two-dimensional computational fluid dynamics (CFD) to predict inlet and nozzle performance, and a one-dimensional cycle code for the combustor. Stability and control are handled using a combination of tail and ballast sizing. Optimization is performed by varying vehicle geometric variables using a numerical algorithm to maximize performance (i.e., range) for a specified vehicle gross weight, length, width and height, and accounts for both airbreathing acceleration and cruise phases of flight along a specified trajectory (i.e., Mach

Received 25 June 2000; revision received 1 May 2001; accepted for publication 19 May 2001.

*Boeing Senior Technical Fellow, Chief Scientist of Hypersonics. Senior Member AIAA.

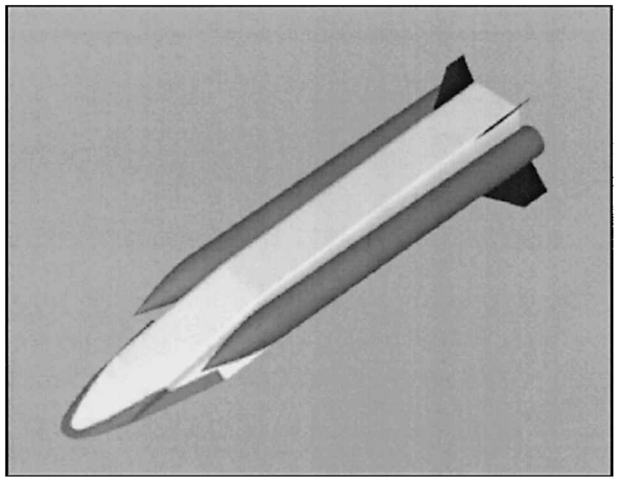

Fig. 1 Scramjet-powered hypersonic cruise missile concept.

vs altitude). A significant body of related work has been performed by other researchers and reported in the literature.[3–7]

The design optimization process described was applied to a baseline Mach 6–7 cruise missile concept illustrated in Fig. 1. Maximum speed and other missile requirements were established by the Defense Advanced Research Projects Agency (DARPA) Affordable Rapid Response Missile Demonstrator (ARRMD) program[8] for which this missile concept was developed. Design constraints of maximum length, width, height and weight were also established by the ARRMD program. Operationally, the missile is boosted to Mach 4.5 using solid rocket motors, then accelerated to cruise speed using an endothermic hydrocarbon-fueled scramjet developed under the U.S. Air Force HyTech program.[9] The scramjet flowpath was separately optimized for specific impulse over a Mach number range of 4–8 as part of the HyTech program, and then, for this work, was optimized in conjunction with the missile only in terms of placement and orientation on the missile. The primary result of optimizing the ARRMD missile configuration was a 46% range increase over the baseline configuration.

What follows is a description of the overall MDO process developed, information on the associated component models, and how they interact with each other. Trends in design parameters for the optimized vehicle, quantitative examples that support the need for hypersonic vehicle MDO, and some of the underlying physics that drove the vehicle to its optimum configuration will also be discussed.

MDO Approach

The fundamental approach employed in this work included creation of a parametric configuration geometry model; development of physics models for aerodynamics, propulsion, stability, control, and mass properties as functions of geometric variables; then use of trajectory analysis to assess vehicle performance (i.e., airbreathing range), and a numerical optimization algorithm to search and find the set of geometric variables that maximize performance.

For optimization five independent geometric variables were selected for their ability to influence longitudinal trim. The first was nose angle, which primarily influences vehicle volume and drag. The second was engine axial location, which influences propulsive thrust, lift, and pitching moment, as well as vehicle mass distribution and volume. Also selected was engine cant, which also profoundly influences propulsive forces and moments as well as vehicle volume, and finally chine length, which influences vehicle lift. The body chines are lifting surfaces outboard of the main fuselage lying in the so-called "forebody ground plane," and nose angle and engine cant are defined relative to the ground plane. These geometric variables are illustrated schematically in Fig. 2.

Vehicle analysis to predict range is performed using models constructed for each vehicle component and functional discipline. Models, described in detail next, were developed to calculate aerodynamic and propulsive forces and moments, plus vehicle mass properties, as functions of the five geometric variables. The approach for each model was tailored to the physics being modeled and to the need for adequate fidelity and fast computational time required for practical optimization. The analysis process, interactions between analysis models, and integration with the optimization algorithm are illustrated in the flow diagram of Fig. 3. The optimization objective of this work was to maximize vehicle airbreathing range (the sum of acceleration and cruise ranges) under the constraints of vehicle trim (i.e., lift equal weight and moments sum to zero everywhere along the trajectory, and thrust equal drag during cruise), longitudinal stability sufficient for automatic flight control, adequate control power for maneuver, a fixed gross weight, and fixed overall length, width, and height.

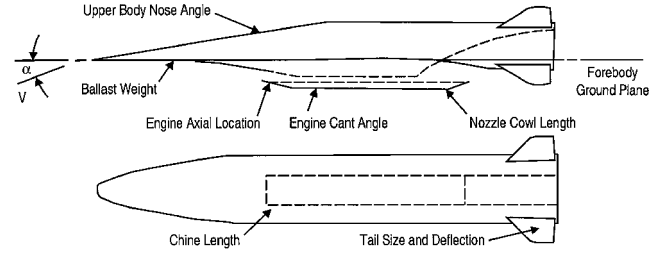

Fig. 2 Independent and dependent configuration variables selected for optimization.

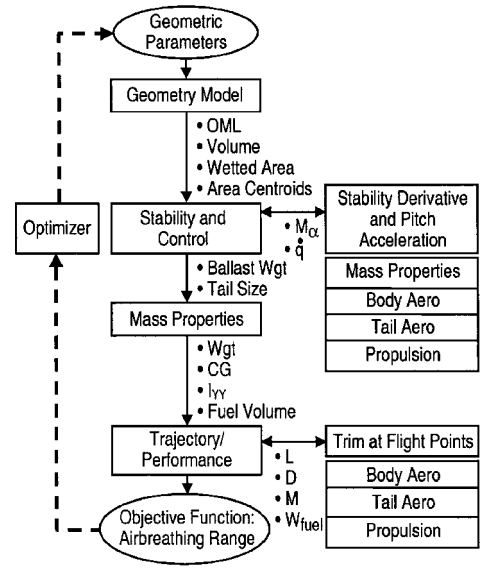

Fig. 3 Analysis flow between disciplines for hypersonic MDO process.

Analysis Models

Geometry Model

The selected vehicle application is a cruise missile, as such it is constrained in length, width, height, and launch weight in order to conform to predefined carriage requirements. Engine width was held constant, as was the internal flowpath from the cowl lip to the combustor exit in order to maintain the applicability of the HyTech propulsion technology database. Using rules to operate within these constraints, the geometry program determined the outer mold lines as a function of the five independent variables and decomposed the geometry into panels for mass properties and aerodynamic calculations. Because of the generally faceted nature of the configuration (illustrated in Fig. 1), it was readily amenable to geometric parameterization. To start, the configuration was divided into 53 rectangular and triangular panels, along natural topologic boundaries, sufficient to accurately capture geometric details. To minimize panels, rectangles were used to model large planar areas, and triangles were used to model areas with curvature.

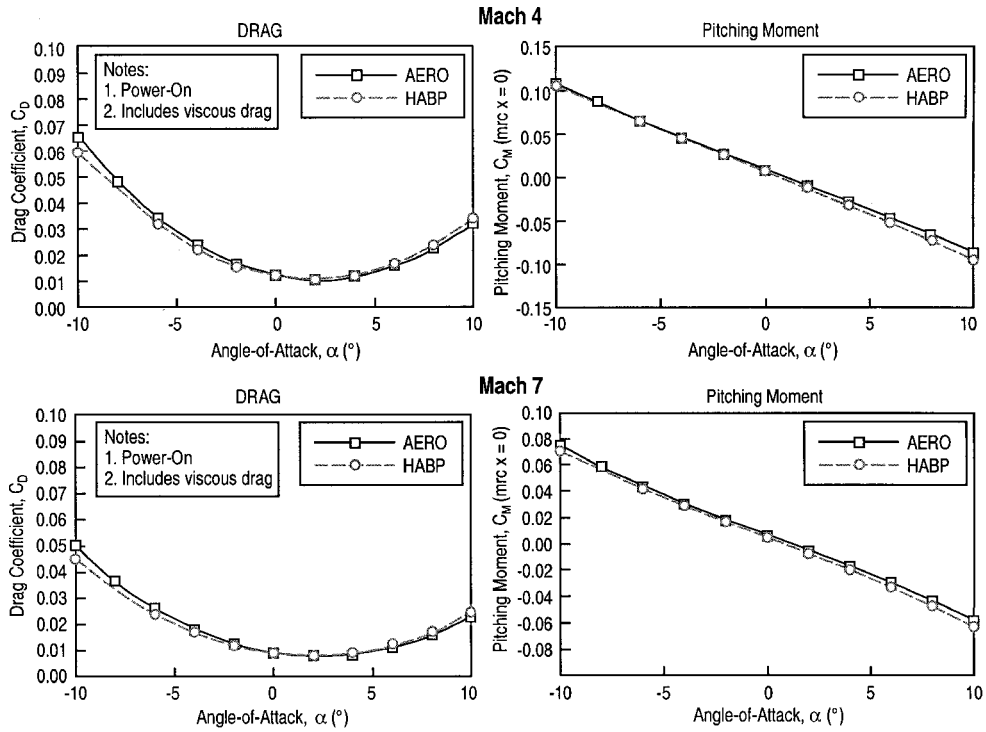

Fig. 4 Drag and pitching moment compare well between MDO aerodynamics model and HABP at all mach numbers.

From the discretized geometry model parametric variations of the geometry were created numerically using a set of geometric construction rules, subject to constraints. For example, when the engine cant angle was changed the body upper surface was rotated with it to maintain the height constraint (i.e., they remained parallel). The most complex rules were associated with the inlet geometry. For example, the internal convergence angle and length of the inlet were maintained at a constant value to preserve HyTech-tested characteristics related to inlet starting and operability. In addition, the engine cowl lip position was translated along a locus of points corresponding to the bow shock line with which the inlet was originally designed. This rule, although somewhat arbitrary, was intended to preserve certain shock-on-lip characteristics that impact the mechanical design of the inlet; it has the residual effect of reducing the capture height of the inlet as the engine is moved forward.

From the spatial distribution of panels (i.e., panel vertex spatial coordinates), vehicle volume, surface wetted area, centroid of surface area, and individual panel normal vectors were calculated using straightforward geometric analyses. Volume, area, and centroids are used in subsequent mass property analysis, whereas panel unit normal vectors are required for aerodynamic analysis to be described next.

Aerodynamic Model

The surface pressure on each vehicle body panel defined by the geometry model is predicted using tangent wedge oblique shock theory or Prandtl–Meyer theory,[10] depending upon whether a panel is angled toward the freestream flow or subtends it, respectively. These methods generally yield good agreement with actual pressures when freestream Mach number is greater than or equal to about four, and the vehicle geometry is more or less planar in its gross features. Both of these requirements were satisfied in the current study. The angle of each panel relative to the freestream flow, required to execute the pressure methods, was derived from the vector dot product between each panel normal vector and the freestream velocity vector.

Viscous drag was predicted from computed vehicle wetted area and a table of average skin-friction coefficients vs Mach number and altitude. A single coefficient of friction was used for the entire vehicle, derived from a detailed analysis of the baseline configuration. Analysis was based on all-turbulent boundary-layer flow—a conservative assumption. This simple approach was deemed adequate for this study because vehicle constraints (vehicle length, width, and height) limited both wetted area variation and the ability to take full advantage of the tradeoff between viscous and pressure drag.

Vehicle base drag was not included in this study. Because optimization was performed for scramjet-powered flight only, nozzle base areas were assumed to be pressurized at ambient levels as a result of underexpanded engine plume interaction effects; a result based on space-shuttle plume interaction data.

Tail force and moment contributions were evaluated external to the aerodynamic model using the Hypersonic Arbitrary Body Program (HABP),[11] then added to the model as tabulated data vs Mach, angle of attack, and tail-deflection angle. This approach is adequate because tail geometry is maintained fixed in this study, with the exception of planform area, which is photographically scaled to meet stability and control requirements.

To illustrate the validity of this fairly simple aerodynamic methodology, a comparison was made between the predictions of this method and a more detailed engineering analysis using HABP on a CAD-lofted version of the optimized vehicle geometry. Comparisons of drag and pitching-moment coefficients between the two methods at Machs four and seven are presented in Fig. 4, where it is seen that the predictions of both coefficients vary by at most 8% at the largest angles of attack evaluated (which exceed those required for trajectory analysis by about 5 deg). This positive result was expected because the hypersonic pressure prediction methods used here are essentially the same as a subset of those in HABP. The comparison was performed principally to verify the function of the pressure methods implemented in the aerodynamic model of this study.

Propulsion Model

The propulsion system used on the missile concept is based on hydrocarbon scramjet technology developed by Pratt & Whitney under the Air Force Research Laboratory (AFRL) Hypersonic Scramjet Engine Technology (HySET) program (HySET is a hydrocarbon scramjet technology development program funded by the U.S. Air Force's HyTech Office). The baseline engine was designed to operate from Mach 4 to 8 and had been optimized for specific impulse at a reference angle of attack over the flight envelope. This earlier

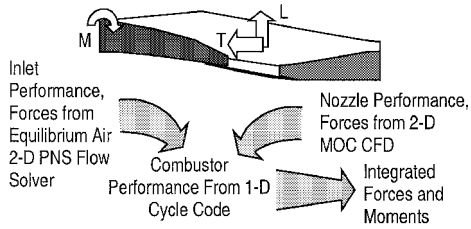

Fig. 5 Nose-to-tail CFD analysis of engine flowpath used to build propulsion model.

optimization involved trade studies, which explored the impact of inlet geometry and engine cowl length on thrust performance. During the current optimization process, the internal lines of the engine from the cowl lip to the end of the combustor were held constant to preserve the operability and efficiency characteristics of the engine.

Engine performance was determined by means of three separate fluid dynamics codes. Inlet analysis was conducted using the SCRAMP/SCRINT[12] two-dimensional Parabolized Navier–Stokes solver. Isolator and combustor analysis was performed using the Pratt and Whitney one-dimensional cycle code RASCAL and nozzle analysis by the two-dimensional method of characteristics flow solver TDK.[13] As illustrated in Fig. 5, propulsive thrust, lift, and pitching moment were derived from vehicle nose to tail across the width of the flowpath using these codes. An analytic propulsion model was then constructed from the detailed analysis results using response surface curve-fitting techniques. Aerodynamic analysis was performed outside the propulsion boundaries, including the engine cowl external surface.

Stability and Control Model

The stability and control model essentially sizes vehicle nose ballast weight and tail planform area to achieve adequate longitudinal stability (i.e., acceptable instability for automatic control) and control power. Sizing of these components is accomplished in the model by evaluating two quantities: first, the longitudinal stability derivative M_α, which is the partial derivative of pitching moment with respect to angle of attack, and second, pitch acceleration rate $\dot{q}$. Forces and moments from the aerodynamic and propulsion models are used to evaluate these terms.

The longitudinal stability derivative M_α is an important parameter for both statically stable and unstable flying machines. For vehicles designed to be statically unstable, the time it takes to double pitch amplitude cannot fall below a certain critical value for a feedback control system to maintain stable flight. Because time-to-double T_2 is proportional to $\sqrt{(I_{YY}/M_\alpha)}$, it is clear that M_α must not exceed a certain magnitude to keep T_2 above its critical value. In the stability and control model T_2 is evaluated at the critical trajectory point where flight dynamic pressure is a maximum, then nose ballast weight is sized to adjust vehicle center of gravity until the T_2 requirement is satisfied.

Next, tail size is evaluated at three critical flight maneuver points (and at several angles of attack at each point) in the trajectory, then modified, if needed, to meet a pitch acceleration rate requirement. Pitch acceleration is a good measure of control power available for maintaining dynamic stability and for maneuvering. If the tail size is modified, then stability is reevaluated, ballast resized, and tail size reevaluated, etc. This analysis loop, illustrated in Fig. 6, is iterated to convergence. Ballast and tail size then become inputs to the mass properties model.

Mass Properties Model

The mass properties model utilizes incremental engineering analysis to evaluate vehicle weight, volume, center of gravity, and pitch moment of inertia. This approach requires an initial detailed mass properties analysis of the baseline vehicle being optimized, then mass properties are incremented relative to the baseline values as functions of the independent variables. More specifically, from changes in vehicle internal volume wetted surface area and centroid

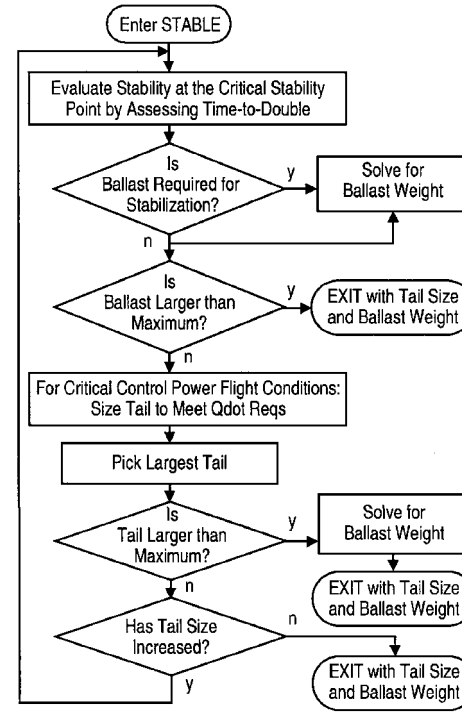

Fig. 6 Analysis flow diagram and iteration loop for stability and control model.

of surface area evaluated by the geometry model; plus ballast and tail size evaluated by the stability model; and finally engine weight, center of gravity, and inertia evaluated by the propulsion model; total vehicle weight, fuel load, center of gravity, and pitch inertia increments are calculated using elementary engineering relationships. As an example, vehicle structural weight was taken to be proportional to outer mold line wetted area. Though generally not an extremely accurate assumption, the vehicle length, width, and height constraints of this study limited area variations enough to make this weight proportionality assumption reasonably valid. Vehicle gross weight was constrained to be less than or equal to a fixed value in this study; therefore, fuel load was taken to be the smaller of the gross-weight-limited fuel weight and the volume-limited fuel weight.

The mass properties model was validated by performing a detailed mass properties analysis of the optimized vehicle. Comparison was excellent, with both gross weight and center of gravity agreeing to within 1% between methods.

Trajectory Analysis

Trajectory analysis was performed by first-order integration of the equations of motion and fuel flow rate between discrete Mach number and altitude points along a prescribed trajectory. First-order integration was determined to be sufficiently accurate because of relatively low accelerations experienced by the vehicle. Trajectory analysis was initiated at the end of rocket boost and included air-breathing acceleration and cruise legs. The vehicle was trimmed in lift and pitching moment at each point along the acceleration leg and in lift, pitching moment, and thrust along the cruise leg. Angle of attack, tail-deflection angle, and throttle setting were iterated to effect trim. Also, vehicle weight was adjusted for centrifugal relief effects as a function of velocity and Earth's radius. The trajectory analysis routine was validated by comparing results with those predicted by optimal trajectories by implicit simulation (OTIS)[14] along an identical trajectory; they differed by only 2% in range.

Optimization

Numerical optimization was used to determine the combination of five geometric variables that maximized airbreathing range. Geometric variables were constrained to be within physically reasonable bounds or within the ranges for which they were evaluated

to build models in the case of the three engine flowpath variables. Overall vehicle length, width, height, and gross weight were also constrained to remain at baseline values. The nonlinear simplex method of Nelder and Mead[15] was used for optimization. The value of the simplex method is two-fold: only the objective function, not function derivatives, require evaluation, and the method handles a relatively large number of independent variables efficiently. Applied in this case, the simplex method required 200–300 iteration cycles for optimizer convergence, taking approximately five minutes of CPU time on a silicon graphics octane work station.

Results and Discussion

The result of the optimization was a much different vehicle than the baseline. Key changes include 1) engine moved forward by 6% of vehicle length, 2) engine cant reduced by 2 deg, 3) engine cowl length reduced by 5% of vehicle length, and 4) chine length reduced by 82% of vehicle length.

Checks of the response surface propulsion model against nose-to-tail analysis of the optimized configuration indicated that the model underpredicted propulsive lift and pitching moment in the vicinity of the optimized design. However, the model provided sufficiently accurate trending for the optimizer to identify desired force and moment characteristics and the most favorable region of design space. A brief parametric study showed that increasing the engine cowl length by 22% of vehicle length would produce the optimum propulsive lift and moment values.

The optimized vehicle, flying the same Mach-dynamic pressure profile as the baseline, achieved 46% greater airbreathing range. In the acceleration portion of the mission, the optimized vehicle showed up to a 9% improvement in effective specific impulse $[(T-D)/w_f]$ over the baseline. Also, trim drag was reduced by 13% overall. The configuration benefits resulting from geometry changes were many. First, the more forward engine location resulted in improved vehicle center of gravity, hence reduced ballast requirement and greater fuselage volume, both of which contributed to increasing vehicle fuel load capacity by 17%. The virtual elimination of the chine resulted in lower vehicle lift, allowing the optimized vehicle to fly at higher angles of attack and reap the thrust benefits of increased inlet air capture and higher lift-to-drag ratio (L/D). In fact, L/D was improved for both high dynamic pressure (Q) acceleration and low-Q cruise, with the optimized vehicle flying slightly to the left of peak L/D during acceleration and slightly to the right during cruise—an interesting balance achieved through optimization. Optimized vehicle longitudinal balance was also improved; therefore, tail deflections and trim drag were reduced commensurately.

As an interesting aside, subsequent trajectory optimization for the optimized vehicle using the OTIS code yielded an additional 52% increase in range relative to that of the optimized vehicle along its fixed trajectory. This is an additional benefit that can be derived from high-performance configurations given the capability of trajectory optimization codes such as OTIS to capitalize on the many operational degrees of freedom available for improving flight performance.

It is instructive here to point out an aerodynamic lesson learned on this project. Wind-tunnel testing and CFD analysis were performed on the optimized vehicle, providing a valuable opportunity to compare engineering prediction methods with high-fidelity test and analysis results. In doing so, it was found that HABP-like engineering methods substantially overpredicted lower surface pressures on the aft regions of the vehicle. By careful examination of this result, it was concluded that the extremely low aspect ratio (approximately 0.1) of the missile configuration led to dominant three-dimensional flow effects on the rear portions of the vehicle. However, the primary impact of aerodynamic differences was on vehicle stability, not flight performance. For example, vehicle range was reduced by only 6% based on wind-tunnel aerodynamics, but vehicle instability was increased by 120% in terms of negative static margin, decreasing the maximum flight dynamic pressure at which the missile could operate by a factor of four. Subsequent chine lengthening and reshaping led to tripling the maximum operational dynamic pressure, achieving 75% of design requirement and essentially recovering vehicle performance and operation to optimized levels.

Table 1 Range sensitivities to the five vehicle design parameters

Parameter	Derivative
$\partial R/\partial\lvert\theta_{\text{nose}}\rvert$	+64 nm/deg
$\partial R/\partial\lvert x_{\text{eng}}\rvert$	+47 nm/ft
$\partial R/\partial\lvert\theta_{\text{cant}}\rvert$	−92 nm/deg
$\partial R/\partial\lvert\ell_{\text{cowl}}\rvert$	+113 nm/ft
$\partial R/\partial\lvert\ell_{\text{chine}}\rvert$	+25 nm/ft

The causes and effects of the optimization results were numerous and highly interrelated, making them difficult or impossible to arrive at using an uncoupled, single-variable-at-a-time trade study approach. Some of the results were also quite counterintuitive. To illustrate the difficulty of using a traditional trade study approach for hypersonic vehicle design, sensitivities of vehicle range to each of the independent design parameters were generated numerically for the baseline vehicle. The resulting partial derivatives are presented in Table 1. A positive sign indicates that the initial sensitivity derivative points in the direction of the optimized configuration for that parameter, and a negative sign indicates the opposite. As indicated by the results, one of the more powerful single variables, engine cant, has a sensitivity trend at the baseline design point opposite the final optimum. This result illustrates the synergy that can be achieved through interaction among interdependent design parameters. This is a hallmark of MDO—a variation that might be detrimental by itself can be beneficial when working in concert with many coupled variations.

To illustrate the claimed importance of scramjet propulsive lift and pitching moment to vehicle trim, stability, and overall performance, two examples will be given. The first is to simply compare the lifts and pitching moments generated by the body and engine flowpath (in nose-to-tail force accounting) for the optimized vehicle to illustrate the relative contribution of each to total vehicle forces. For example, at a Mach 4.5 trimmed flight point propulsive lift is 40% of aerodynamic lift, and propulsive moment (about the center of gravity) is 50% of the aerodynamic moment. On the other end of the speed spectrum at Mach 6.5, propulsive lift is 13% of aerodynamic lift, and propulsive moment is 83% of the aerodynamic moment. In the latter case the counteracting engine moment almost balances the aerodynamic moment to trim the vehicle. Clearly, the highly integrated engine is a significant contributor to vehicle lift and pitching moment and can therefore influence drag due to lift and trim drag.

The second example illustrates the benefit of propulsive lift by analyzing the Breguet range equation. To start, the range equation is modified to account for a propulsion system that generates net lift. The derivation is applicable to any aeropropulsion force accounting system (e.g., nose-to-tail or cowl-to-tail) as long as the division between aerodynamic and propulsive forces is consistent.

The most basic form of the Breguet range equation can be written

$$R = \int \mathrm{d}x = \int V\,\mathrm{d}t = V\int \frac{\mathrm{d}W}{\dot{W}} = -V\int_{W_i}^{W_f} \frac{\mathrm{d}W}{w_f} \tag{1}$$

Next, from the definitions of specific impulse,

$$I_{\text{sp}} \equiv T/w_f \tag{2}$$

and weight corrected for centrifugal relief,

$$W' \equiv \left(1 - V^2/gr_E\right)W \equiv KW \tag{3}$$

where the force relationships for equilibrium cruise flight are

$$L = W' - L_p \tag{4}$$

$$T = D \tag{5}$$

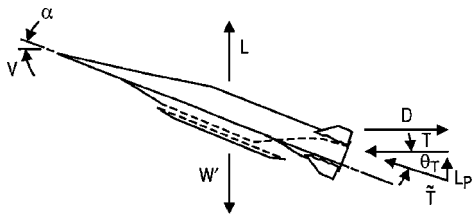

Fig. 7 Definition of aerodynamic and propulsion forces.

the range equation becomes

$$R = -\frac{V}{K} I_{\text{sp}} \left(\frac{L}{D}\right) \int_{\tilde{W}_i}^{\tilde{W}_f} \frac{\mathrm{d}\tilde{W}}{\tilde{W}} = \frac{V}{K} I_{\text{sp}} \left(\frac{L}{D}\right) \ell n \left(\frac{\tilde{W}_i}{\tilde{W}_f}\right) \tag{6}$$

Refer to Fig. 7 for a schematic description of vehicle forces.

To arrive at the modified form of the range relationship given in Eq. (6), L/D and I_{sp} are assumed constant during cruise, and integration must be performed over the range of required aerodynamic lift (as opposed to weight in the classical derivation) between the beginning and end of cruise, which is related to weight and propulsive lift as given in Eq. (4), but now defined as $\tilde{W}$, where

$$\tilde{W} \equiv L = W' - L_p = KW - L_p \tag{7}$$

Though L/D and I_{sp} are here assumed constant to illustrate the benefits of propulsive lift, the assumptions are not too far from true for the subject missile of this work. For example, during cruise missile weight (i.e., lift requirement) changes by only 14% as a result of fuel consumption, and L/D varies by no more than 6%.

A valuable prediction that can be derived from the modified Breguet range equation is the optimum split between lift generated aerodynamically and propulsively. Returning to Eqs. (1–5) and Fig. 7, the differential of range written in terms of fuel flow rate can be expressed as

$$\delta R = \frac{-V \delta W}{wf} = \frac{-V \delta W}{W' - T \sin\theta_T} \left(\frac{L}{D}\right) \tilde{I}_{\text{sp}} \cos\theta_T \tag{8}$$

where

$$\tilde{I}_{\text{sp}} \equiv \tilde{T} / w_f \tag{9}$$

If it is assumed, ideally, that the thrust magnitude $\tilde{T}$ can be rotated to any thrust vector angle θ_T without affecting thrust magnitude, then Eq. (8) can be differentiated with respect to θ_T, and the result set equal to zero to find the thrust vector angle that maximizes range for fixed L/D and $\tilde{I}_{\text{sp}}$. Carrying out the math (subject to equilibrium-cruise force equalities), the optimum thrust vector angle is found to be related to cruise L/D by

$$(\theta_T)_{\text{opt}} = \tan^{-1}[1/(L/D)] \tag{10}$$

Though this analysis is simplistic—in reality $\tilde{T}$ will likely vary with θ_T and $\tilde{I}_{\text{sp}}$ with w_f—it does indicate a vehicle performance benefit from propulsive lift, and the optimum propulsive lift is inversely proportional to L/D. From an intuitive perspective the lower drag due to lift achieved by reducing the aerodynamic lift requirement results in an effective L/D (W'/D) that exceeds the actual L/D, improving range performance.

This theory was tested out on the optimized vehicle of this study by comparing the optimum thrust vector angle with the actual value at cruise. Doing so, the actual cruise value of θ_T was about 7 deg larger than the optimum value predicted by Eq. (10). In this case effective L/D was 14% higher than actual L/D. The former indicates that perhaps additional, less constrained optimization might achieve even greater performance increases. Computational experimentation provided additional evidence for this possibility.

As shown by these two examples, vehicle performance can be influenced favorably by taking advantage of propulsive pitching moment and lift to reduce trim drag and drag due to lift, respectively. Vehicle optimization via MDO can then be used to capitalize on these and many other synergistic system interactions.

Conclusions

A multidisciplinary design optimization process has been developed for hypersonic vehicles and successfully applied to a hypersonic missile concept. The process accounts for several highly interdependent disciplines, namely aerodynamics, propulsion, stability and control, mass properties, and flight performance. Each of the discipline models has been described in limited detail.

Employing the MDO process produced an optimized configuration with a dramatic 46% range increase over an initial baseline vehicle. Such a large improvement is caused, in part, by the relatively low performance of the baseline configuration; this highlights the formidable challenge of hypersonic vehicle design, where high levels of component integration and optimization are required to achieve acceptable performance. Generally, the MDO process was able to capture the synergies achievable between system components and exploit the physics inherent in highly integrated engine-airframe designs employing bottom-mounted scramjet engines. Specifically, the optimized vehicle realized range improvement through 1) increased propellant mass fraction, 2) increased operational angle of attack, which increased thrust and L/D, and 3) reduced residual vehicle pitching moment, hence trim drag. The latter two contributed to increased vehicle effective I_{sp}.

The inclusion of vehicle trim as a factor in assessing range performance results in a different optimum configuration than when the propulsion system is optimized alone. Propulsive lift and pitching moment have a profound influence on the actual angle of attack at which the vehicle flies and thus on the performance of the propulsion system. A clear result of this study is that hypersonic propulsion system optimization activities must include the impact of vehicle trim. A few analytical examples were given to help support these assertions.

For complex, highly coupled systems, such as hypersonic vehicles, it is believed that an automated MDO process such as the one described is essential for realizing the performance potential of the individual technologies comprising the system; intuition and classical design techniques can go only so far in achieving this end.

Continued work will focus on generating high-fidelity propulsion models using design of experiments, response surfaces, and CFD analysis methods together in more efficient and effective ways; employing more sophisticated analysis routines to the degree they add value and are practical; and evolving the process to be more generally applicable to a broad range of hypersonic vehicles and configuration classes.

Acknowledgments

I would like to acknowledge the dedicated experts that helped make my vision of hypersonic vehicle optimization a reality: Jeff Weir of Boeing for aerodynamics and geometry modeling; Mark Nugent of Boeing for the stability and control model; Jonas Surdenas and Rena Beyale of Boeing for the mass properties model; and Alan Drake, Richard Hawkins, and Thomas Verdi of Pratt and Whitney for the propulsion model. They worked tirelessly to meet nearly impossible deadlines, and for that I am grateful.

References

[1] Waldman, B. J., and Harsha, P. T., "The National Aero-Space Plane Program," AIAA Paper 90-5252, Oct. 1990.

[2] Bowcutt, K. G., "Hypersonic Aircraft Optimization Including Aerodynamic, Propulsion and Trim Effects," AIAA Paper 92-5055, Jan. 1992.

[3] Baysal, O., and Eleshaky, M. E., "Aerodynamic Design Optimization Using Sensitivity Analysis and Computational Fluid Dynamics," *AIAA Journal*, Vol. 30, No. 3, 1992, pp. 718–725.

[4] O'Neill, M. K., and Lewis, M. J., "Design Tradeoffs on Scramjet Engine Integrated Hypersonic Waverider Vehicles," *Journal of Aircraft*, Vol. 30, No. 6, 1993, pp. 943–952.

[5] McQuade, P. D., Eberhardt, S., and Livine, E., "CFD-Based Aerodynamic Approximation Concepts Optimization of a Two-Dimensional Scramjet Vehicle," *Journal of Aircraft*, Vol. 32, No. 2, 1995, pp. 262–269.

[6]Bogar, T. J., Alberico, J. F., Johnson, D. B., Espinosa, A. M., and Lockwood, M. K., "Dual-Fuel Lifting Body Configuration Development," AIAA Paper 96-4592, Nov. 1996.

[7]Takashima, N., and Lewis, M. J., "Optimization of Waverider-Based Hypersonic Cruise Vehicles with Off-Design Considerations," *Journal of Aircraft*, Vol. 36, No. 1, 1999, pp. 235–245.

[8]Wall, R., "DARPA Selects Mach 6+ Missile," *Aviation Week and Space Technology*, Vol. 151, No. 15, 1999, p. 96.

[9]Reddecliff, J. M., and Weber, J. W., "Development and Demonstration of a Hydrocarbon Scramjet Propulsion System," AIAA Paper 98-1613, April 1998.

[10]Anderson, J. D., Jr., *Modern Compressible Flow: With Historical Perspective*, McGraw–Hill, New York, 1982, pp. 88–113.

[11]Gentry, A. E., Smyth, D. N., and Oliver, W. R., "The Mark IV Supersonic–Hypersonic Arbitrary-Body Program," AFFDL-TR-73-159, Vols. 1, 2, and 3, Nov. 1973.

[12]Krawczyk, W. J., Harris, T. B., and Rajendran, N., "Progress in Development of Parabolized Navier–Stokes Technology for External and Internal Supersonic Flows," AIAA Paper 89-1828, June 1989.

[13]Dunn, S. S., and Coats, D. E., "Nozzle Performance Predictions Using the TDK 97 Code," AIAA Paper 97-2807, July 1997.

[14]Paris, S. W., Hargraves, C. R., and Vlases, W. G., "OTIS (Optimal Trajectories by Implicit Simulation) Past, Present and Future," AIAA Paper 92-4530, Aug. 1992.

[15]Nelder, J. A., and Mead, R., "A Simplex Method for Function Minimization," *Computer Journal*, Vol. 7, No. 4, 1965, pp. 308–313.